Fluorescence and Ultraviolet Absorption Spectra, and the Structure and Vibrations of 1,2,3,4-Tetrahydronaphthalene in Its $S_1(\pi,\pi^*)$ State

Juan Yang, Martin Wagner, and Jaan Laane*

Department of Chemistry, Texas A&M University, College Station, Texas 77843-3255

Received: May 15, 2007; In Final Form: June 18, 2007

The ultraviolet absorption spectra in the static vapor phase and the laser induced fluorescence spectra (both fluorescence excitation and single vibronic level fluorescence spectra) of jet-cooled 1,2,3,4-tetrahydronaphthalene have been used along with theoretical calculations to assign many of the vibronic levels in the $S_1(\pi,\pi^*)$ state. These have been compared to the corresponding vibrational levels for the S_0 ground state. Analysis of the upper states of the ring-twisting vibration ν_{31} and three other low-frequency modes has allowed us to construct an energy map of the lowest vibrational quantum states for both S_0 and S_1. The molecule is highly twisted in both electronic states with high barriers to planarity, which are calculated to be 4811 cm^{-1} for S_0 and 5100 cm^{-1} for S_1. However, the experimental data show that the barrier should be lower in the S_1 state.

Introduction

We have previously reported[1,2] the spectra and a two-dimensional analysis of the ring-twisting and ring-bending vibrations of cyclohexene (CHX). The calculated potential energy surface had a barrier to planarity of 4700 cm^{-1} with the lowest energy conformations at twist angles of ±39°. As was the case for CHX, 1,2,3,4-tetrahydronaphthalene (tetralin or TET) is also expected to have twisted C_2 symmetry with a very high barrier to planarity, and TET is the focus of our present investigation.

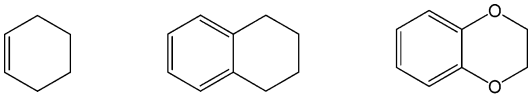

CHX TET 14BZD

The complete vibrational assignments of TET and the related molecule 1,4-benzodioxane (14BZD) in the electronic ground state have already been published.[3] We have also reported the laser induced fluorescence (LIF) and ultraviolet (UV) absorption study of 14BZD.[4] In the present study we report the UV absorption spectra and the supersonic jet-cooled LIF spectra, including both fluorescence excitation (FES) and single vibronic level fluorescence (SVLF) spectra of TET. The LIF spectra of this molecule have previously been studied by the Chowdhury group,[5] who reported the molecule to be twisted and who made rough estimates of the barrier to interconversion. In our work we have been able to obtain improved spectra and to revise many of the earlier assignments. Our focus has been primarily on the low-frequency out-of-plane modes whose potential energy surfaces determine the structure of the molecule. One-dimensional potential functions for the ring-twisting mode for both the S_0 ground and $S_1(\pi,\pi^*)$ excited states will be reported. We will also present high level theoretical calculations for this molecule for both electronic states.

Experimental Methods and Calculations

The 1,2,3,4-tetrahydronaphthalene sample (99% purity) was purchased from Aldrich Chemical Co. and further purified by vacuum distillation. Ultraviolet absorption spectra of tetralin vapor at ambient temperatures were recorded on a Bomem DA8.02 Fourier transform spectrometer using a deuterium lamp source, a quartz beamsplitter, and a silicon detector in the 20 000−50 000 cm^{-1} region. The sample was contained in a 20 cm glass cell with quartz windows. A resolution of 0.25 cm^{-1} was used, and more than 20 000 scans were averaged. The FES and SVLF spectra were recorded using a Continuum Powerlite 9020 Nd:YAG laser which pumped a Continuum Sunlite optical parametric oscillator (OPO) and an FX-1 ultraviolet extension unit. For the FES the laser was scanned under computer control and the fluorescence was detected with a photomultiplier tube whenever resonance with a vibronic level was achieved. For the SVLF study a specific vibronic transition was selected and the fluorescence bands were dispersed using a 0.64 m Jvon Yovin HR-640 monochromator and measured with a CCD detector. FES spectra were obtained at 0.5 cm^{-1} resolution, and SVLF spectra were taken with a spectral resolution of 1 cm^{-1}. Both types of spectra were recorded under supersonic jet-cooled conditions. More details on the laser system are provided elsewhere.[6−10]

Theoretical calculations for the TET S_0 electronic ground state have been reported in our previous work.[3] Excited-state calculations were carried out using the Gaussian 03 package.[11] Bond lengths, bond angles, and vibrational frequencies were calculated for both planar C_{2v} and twisted C_2 structures in the $S_1(\pi,\pi^*)$ excited state. The configuration interaction singles (CIS) method with the 6-311++G(d,p) basis set was used. The twisted C_2 symmetry was calculated to be the lowest energy conformation for the S_1 excited state.

Figure 1 shows the structures of TET for both C_2 and C_{2v} symmetries calculated with the MP2/cc-pVTZ basis set for the S_0 state and with the CIS/6-311++G(d,p) basis set for the $S_1(\pi,\pi^*)$ state. The bond lengths of the benzene ring increase while the bond lengths outside the benzene ring decrease upon the $\pi \rightarrow \pi^*$ excitation, as expected. The twisting angles for C_2 symmetry were calculated to be 31.4° for the S_0 ground state and 29.3° for the S_1 excited state. Table 1 lists the energies calculated with different theories and basis sets for the planar

10.1021/jp073752p CCC: $37.00
Published on Web 08/08/2007

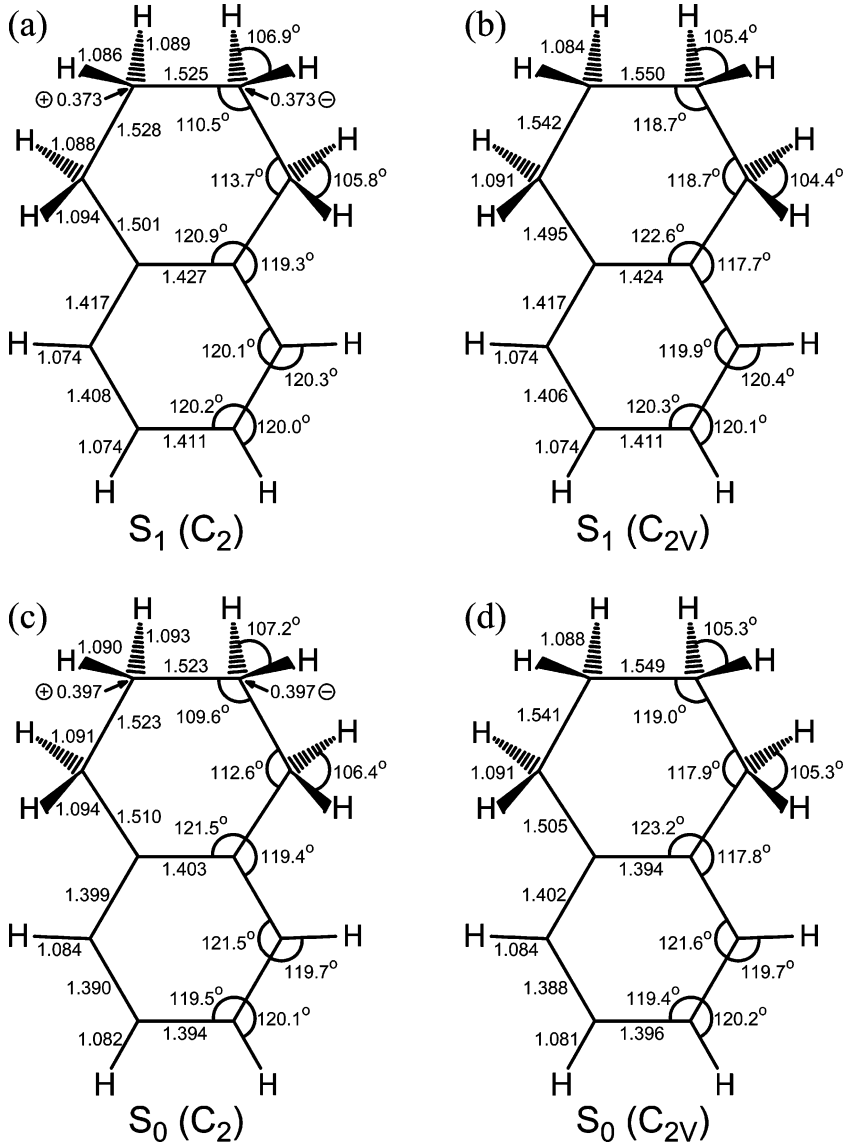

Figure 1. Calculated structures of tetralin for (a) C_2 and (b) C_{2v} symmetries in the $S_1(\pi,\pi^*)$ state from CIS/6-311++G(d,p) calculations and for (c) C_2 and (d) C_{2v} symmetries in the S_0 state from MP2/cc-pVTZ calculations.

TABLE 1: Calculated Relative Energies (cm^{-1}) for Different Structures of Tetralin in Its S_0 Ground and $S_1(\pi,\pi^*)$ Excited States

	S_0				S_1
			MP2		
structure	HF 6-311++G(d,p)	B3LYP 6-311++G(d,p)	6-311++G(d,p)	cc-pVTZ	CIS 6-311++G(d,p)
C_{2v} (planar)	4493	3938	5152	4811	5100
C_s (bent)	992	783	724	716	848
C_2 (twisted)	0	0	0	0	0

(C_{2v}) and bent (C_s) structures of TET in both electronic states relative to the energy minima at the twisted (C_2) conformations.

Table 2 compares the experimental and calculated vibrational frequencies for TET in its S_0 and $S_1(\pi,\pi^*)$ states. A scaling factor of 0.905 for the $S_1(\pi,\pi^*)$ excited state was selected from the average ratio of eight experimental and calculated fundamental frequencies, which are presented in Table 3. The assignments for these eight fundamental bands in the FES spectra are certain and are confirmed by the corresponding SVLF spectra from the various excitation bands, since the intensities in the SVLF spectra are greatest when the transitions involve the same vibration. The scaling factors for these eight fundamental frequencies are all in the range of 0.87−0.93, except the one for the highly anharmonic ring-twisting vibration ν_{31}, which is 0.830 and was not used for averaging. By using the average scaling factor of 0.905, the difference between the experimental and calculated frequencies for all 17 fundamental bands observed in the FES spectra is about 11 cm^{-1}.

For an electronic excited-state calculation the agreement is excellent for TET. It is also better for TET than it was for 14BZD,[4] and this is likely due to complications caused by the oxygen lone pair in the latter molecule.

TABLE 2: Experimental and Calculated Vibrational Frequencies (cm^{-1}) and Assignments for Tetralin in Its S_0 Ground and S_1 Excited States

				ground state (S_0)			excited state (S_1)	
	ν				calcd[b]			calcd[d]
symmetry C_{2v} (C_2)	C_{2v}	C_2	description	expt[a]	C_{2v}	C_2	expt[c]	C_2
A_1 (A)	1	1	C−H sym stretch (ip)	3073[IR]	3069	3069		3048
	2	2	C−H sym stretch (op)	3047[R]	3034	3037		3028
	3	5	CH_2 sym stretch (ip, op′)	2895[R]	2906	2899		2851
	4	6	CH_2 sym stretch (ip, ip′)	2871[R]	2943	2886		2794
	5	7	benzene C−C stretch	1581[R]	1602	1592		1531
	6	8	benzene C−C stretch	1496[IR]	1504	1499		1435
	7	9	CH_2 deformation (ip, ip′)	1463[R]	1507	1481		1469
	8	10	CH_2 deformation (ip, op′)	1440[R]	1460	1453		1417
	9	11	CH_2 wag (op, ip′)	1353[R]	1372	1365		1369
	10	13	benzene C−C stretch	1295[IR]	1336	1309		1640
	11	15	sat. ring (C−C) stretch	1200	1196	1200	1183	1182
	12	16	CH_2 wag (op, op′)	1166[R]	1268	1167		1160
	13	17	C−H wag (op, op′)	1158	1165	1164		1140
	14	19	sat. ring (C−C) stretch	1065[R]	1113	1064		1032
	15	20	C−H wag (op, ip′)	1035	1043	1038	971	968
	16	23	sat. ring (C−C) stretch	864[R]	839	858		835[e]
	17	25	benzene C−C stretch	722	713	723	681	677
	18	27	benzene ring bend	578	584	581	480	489
	19	29	sat. ring bend	428	442	427	417	411
A_2 (A)	20	3	CH_2 asym stretch (op, ip′)	2949[IR]	2948	2946		2894
	21	4	CH_2 asym stretch (op, op′)	2927[R]	2918	2936		2872
	22	12	CH_2 twist (ip, ip′)	1342[R]	1291	1351		1350
	23	14	CH_2 twist (ip, op′)	1251[IR]	1259	1257		1229
	24	18	CH_2 rock (op, op′)	1076[R]	1056	1085		1056
	25	21	C−H wag (op, op′)	1000[R]	969	973		833[e]
	26	22	C−H wag (op, ip′)	868	871	869	677	647
	27	24	CH_2 rock (op, ip′)	817	818	819		800
	28	26	benzene ring bend	700	688	703	521	537
	29	28	benzene ring bend	501	483	504	330	335
	30	30	skeletal twist	298[R]	*i*	301	295	288
	31	31	sat. ring twist	142	125	141	94	103
B_1 (B)	32	32	C−H asym stretch (ip)	3064[IR]	3054	3054		3038
	33	33	C−H asym stretch (op)	3024[IR]	3031	3033		3021
	34	36	CH_2 sym stretch (op, op)	2896[IR]	2905	2905		2853
	35	37	CH_2 sym stretch (op, ip′)	2874[IR]	2927	2885		2789
	36	38	benzene C−C stretch	1598[R]	1618	1618		1449
	37	40	CH_2 deformation (op, ip′)	1456[IR]	1482	1474		1460
	38	39	CH_2 deformation (op, op′)	1448[IR]	1459	1459		1425
	39	41	benzene C−C stretch	1437[IR]	1454	1457		1406
	40	42	CH_2 wag (ip, op′)	1342[R]	1361	1350		1349
	41	43	CH_2 wag (ip, ip′)	1334[L]	1351	1346		1335
	42	45	C−H wag (ip, ip′)	1241[R]	1251	1243		1174
	43	46	sat. ring (C−C) stretch	1189[L]	1204	1184		1146
	44	48	C−H wag (ip, op′)	1112[IR]	1118	1118		1062
	45	49	sat. ring (C−C) stretch	982[R]	1007	981	950	954
	46	53	benzene ring bend	804	854	801		764
	47	55	benzene ring bend	586	728	587[e]	545	547
	48	56	sat. ring bend	450	477	450		407
	49	58	sat. ring bend	339	334	339	327	322
B_2 (B)	50	34	CH_2 asym. stretch (ip, ip′)	2948[R]	2974	2949		2896
	51	35	CH_2 asym. stretch (ip, op′)	2936[IR]	2922	2935		2871
	52	44	CH_2 twist (op, ip′)	1289[R]	1287	1294		1267
	53	47	CH_2 twist (op, op′)	1137[IR]	1219	1142		1104
	54	50	C−H wag (ip, op′)	944[IR]	955	950		728
	55	51	CH_2 rock (ip, ip′)	938[IR]	709	934[e]		908
	56	52	CH_2 rock (ip,op′)	901	910	900	861	875
	57	54	C−H wag (ip, ip′)	741[IR]	749	743	566	613
	58	57	benzene ring bend	436[R]	429	432	270	288
	59	59	sat. ring flap	253[R]	210	255		140
	60	60	sat. ring bend	95	*i*	94	85	93

[a] Experimental frequencies are observed from SVLF spectra unless indicated otherwise. IR, infrared; R, Raman; L, liquid phase infrared. [b] Calculated using the B3LYP/6-311++G(d,p) basis set with Gaussian 03. The scaling factors are 0.985 for frequencies less than 1800 cm^{-1} and 0.964 for frequencies greater than 2800 cm^{-1}. [c] Experimental frequencies are observed from FES spectra. [d] Calculated using the CIS/6-311++G(d,p) basis set with Gaussian 03. The scaling factors are 0.905 for the entire region. [e] Vibrations that are strongly coupled.

TABLE 3: Selected Experimental and Calculated Fundamental Frequencies (cm^{-1}) in the $S_1(\pi,\pi^*)$ Excited State for Tetralin

ν	expt[a]	calcd[b]	scaling factor	scaled freq (SF = 0.905)
17	680.5	748.1	0.910	677.0
18	480.3	540.5	0.889	489.1
19	417.3	454.3	0.919	411.1
28	521.4	593.1	0.879	536.8
29	329.5	370.2	0.890	335.0
30	294.7	317.8	0.927	287.6
31	94.5	113.8	0.830[c]	103.0
49	326.8	355.5	0.919	321.7

[a] Fundamental frequencies obtained from the FES spectra. [b] Unscaled frequencies calculated using the CIS/6-311++G(d,p) basis set with Gaussian 03. [c] Not used in averaging the scaling factors.

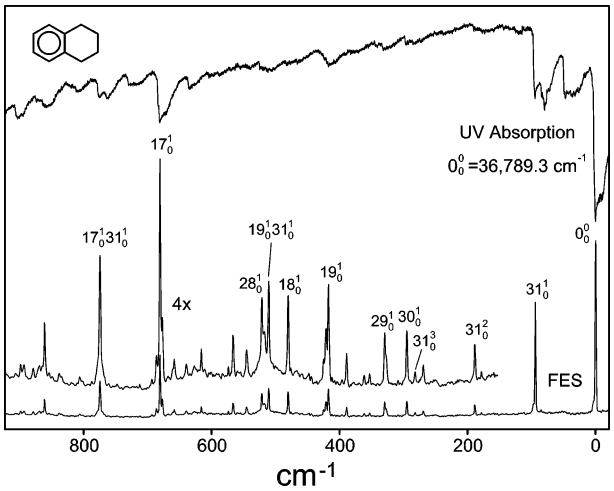

Figure 2. Fluorescence excitation spectra of jet-cooled tetralin and the ultraviolet absorption spectra at ambient temperature in the 0−900 cm^{-1} region.

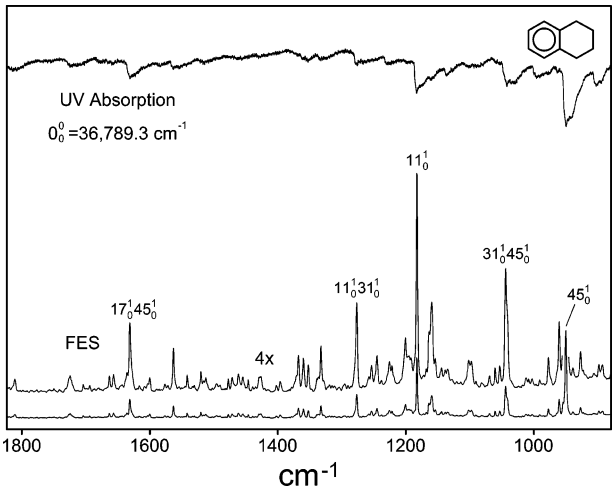

Figure 3. Fluorescence excitation spectra of jet-cooled tetralin and the ultraviolet absorption spectra at ambient temperature in the 900−1800 cm^{-1} region.

Vibrational Hamiltonian

With only limited data for the ring-twisting vibration in both the S_0 and S_1 electronic states, only a one-dimensional analysis for TET could be carried out. The one-dimensional Hamiltonian operator is given by

$$\hat{\mathbf{H}}_{\text{vib}} = -\frac{\hbar^2}{2}\left[\frac{\partial}{\partial\tau} g_{44}(\tau) \frac{\partial}{\partial\tau}\right] + \hat{\mathbf{V}}(\tau) \qquad (1)$$

where τ is the ring-twisting coordinate. The g_{44} expression is the reciprocal reduced mass for the ring-twisting vibration. The methodology and vectors for these calculations are published elsewhere.[12]

Assignments of Spectra

Figures 2 and 3 present the supersonic jet-cooled FES spectra and the room-temperature UV absorption spectra of TET in the 0−900 and 900−1800 cm^{-1} regions, respectively, relative to the electronic band origin 0_0^0 at 36 789.3 cm^{-1}. Table 4 presents the frequencies and assignments for these spectra. Since the observed UV absorption bands are weak and broad due to the weak dipole moment of TET, the assignments in Table 4 are based on the FES frequencies. The FES frequencies and assignments reported by Guchhait et al.[5] are also listed in Table 4 for comparison. These authors numbered the vibrations simply from the lowest frequency to the highest frequency, without considering the symmetry of the molecule. However, we feel that it is more informative to classify the vibrations according to assumed C_{2v} (planar) symmetry and to use the conventional sequence. The previously published FES spectra[5] and assignments only extended to 800 cm^{-1} beyond the 0_0^0 excitation. In our present work, the spectra and assignments up to 2000 cm^{-1} are presented. Also, our FES spectra have a much better signal-to-noise ratio and are at much higher resolution than the spectra reported previously.[5]

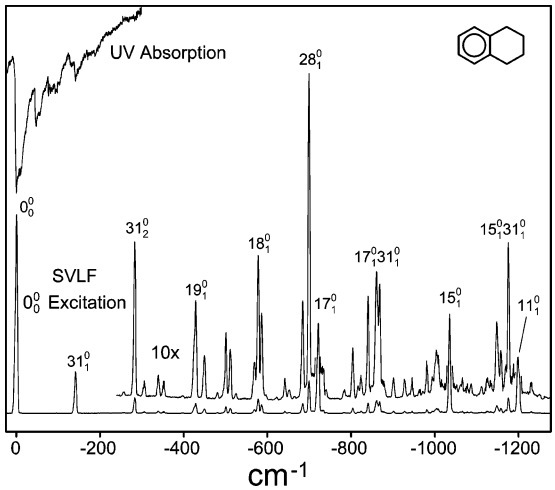

Figure 4. Single vibronic level fluorescence spectra of jet-cooled tetralin with excitation of the 0_0^0 band at 36 789.3 cm^{-1} and the ultraviolet absorption spectra at ambient temperature.

With the help of theoretical calculations, we feel confident about the assignments presented in Table 4. For example, Guchhait et al.[5] did not report the frequency in the S_1 state for the ring-bending vibration (ν_{60}), which is the lowest frequency vibration. We observe this in our FES spectrum as a weak band at 85.1 cm^{-1}. The CIS calculation confirms this assignment with a calculated value of 93 cm^{-1}. In addition, a combination band

TABLE 4: Fluorescence Excitation Spectra (FES), Ultraviolet (UV) Absorption Frequencies (cm^{-1}), and Assignments for Tetralin[a]

this work					GCMC[b]	
FES	UV	calcd[c]	inferred[d]	assignment	FES	assignment
	−283 vw			31_2^0		
	−141 m			31_1^0		
	−95 m, br			60_1^0		
	−57 m, br					
	−47 s			31_1^1		
	−10 s,br			60_1^1		
0.0 vs	0.0 vs			0_0^0	0	0_0^0
	47 s					
	79.5 s					
85.1 w		93		60_0^1		
94.0 vs	94.5 s	103		31_0^1	95	2_0^1
178.0 vw			179.1	$31_0^160_0^1$	179	1_0^2
188.4 m				31_0^2	189	2_0^2
268.9 w		288		58_0^1	270	$1_0^22_0^1$
281.9 vw	282 vw			31_0^3	282	2_0^3
294.7 m	295 vw	288		30_0^1	295	4_0^1
326.8 w		322		49_0^1		
329.5 m	331 w	335		29_0^1	329	3_0^1
353.0 vw			354.0	$58_0^160_0^1$	353	1_0^4
361.6 vw			362.9	$31_0^158_0^1$	363	$1_0^22_0^2$
					375	2_0^4
388.8 m			388.7	$30_0^131_0^1$	390	$4_0^12_0^1$
417.3 s	417 m	411		19_0^1	417	5_0^1
420.9 m			420.8	$31_0^149_0^1$	422	$3_0^12_0^1$
424.8 w			423.5	$29_0^131_0^1$		
					446	$1_0^42_0^1$
480.3 s		489		18_0^1	481	$4_0^12_0^2$
510.8 s	511 w		511.3	$19_0^131_0^1$	511	$5_0^12_0^1/3_0^11_0^2$
517.6 m			517.9	$29_0^131_0^2$		
521.4 s		537		28_0^1	520	$3_0^12_0^2$
545.0 m		547		47_0^1	544	$1_0^42_0^2$
566.3 m		613		57_0^1	566	
573.7 vw			574.3	$18_0^131_0^1$	574	$4_0^12_0^3$
616.1 m			615.4	$28_0^131_0^1$		
639.5 vw			639.0	$31_0^147_0^1$		
658.1 w			660.3	$31_0^157_0^1$		
	671 m					
676.8 m		647		26_0^1		
680.5 vs	681 s	677		17_0^1	679	6_0^1
686.1 w						
	730 w					
	762 m					
770.4 w			770.8	$26_0^131_0^1$		
774.3 s	774 m		774.5	$17_0^131_0^1$	765	7_0^1
778.1 w			777.6	$30_0^231_0^2$		
	808 w					
860.9 ms	861 m	875		56_0^1		
	903 m					
927.2 m			928.1	$19_0^231_0^1$		
939.0 vw	940 m					
	946 m					
950.0 vs	950 s	954		45_0^1		
954.5 m			954.9	$31_0^156_0^1$		
960.4 ms			960.6	18_0^2		
977.3 m		968		15_0^1		
	996 w					
1041.6 m	1042 m		1042.8	28_0^2		
1044.2 s			1044.0	$31_0^145_0^1$		
	1136 w					
1159.8 ms	1160 vw		1160.8	$17_0^118_0^1$		
1164.0 m						
1182.8 vs	1183 m	1182		11_0^1		
1200.8 m			1201.9	$17_0^128_0^1$		
1276.8 ms	1277 w		1276.8	$11_0^131_0^1$		
1332.7 m	1333 w					
1352.5 w	1354 w					
1360.0 m			1361.0	17_0^2		

TABLE 4 (Continued)

this work					GCMC[b]	
FES	UV	calcd[c]	inferred[d]	assignment	FES	assignment
1367.8 m			1367.3	$19_0^1 45_0^1$		
1563.1 m			1563.0	28_0^3		
1631.3 ms	1631 m		1630.5	$17_0^1 45_0^1$		
1810.9 w			1810.9	$45_0^1 56_0^1$		
1863.1 w			1863.3	$11_0^1 17_0^1$		
1898.8 w	1899 w		1900.0	45_0^2		
	2133 w		2132.8	$11_0^1 45_0^1$		

[a] Abbreviations: s, strong; m, medium; w, weak; v, very; br, broad. [b] From ref 5. [c] Calculated using the CIS/6-311++G(d,p) basis set with Gaussian 03. [d] Inferred combination frequencies are based on assignments of individual vibrations.

$31_0^1 60_0^1$ at 178.0 cm^{-1} was also observed with 31_0^1 (94.0 cm^{-1}), further verifying the assignment for ν_{60}.

Figure 4 shows the SVLF spectra with excitation of the 0_0^0 band at 36 789.3 cm^{-1}. The frequencies and assignments for these spectra are given in Table 5 and compared to the fundamental frequencies obtained from the vapor IR and vapor Raman spectra we published previously.[3] Figure 5 shows the SVLF spectra with excitation of the 31_0^1 band at 94.5 cm^{-1} higher than the 0_0^0 band. The UV absorption spectra at ambient temperatures are also shown. The SVLF spectra were recorded from 13 different excitation bands including 0_0^0 and 31_0^1. The frequencies and assignments from eight fundamental excitations are summarized in Table 6. The strongest bands shown in these SVLF spectra always correspond to transitions to the ground-state levels of the same vibration as the excitation. For example, in the SVLF spectra with excitation of the 18_0^1 band at 480.3 cm^{-1} and of the 28_0^1 band at 521.4 cm^{-1}, the strongest bands are observed at 579 and 701 cm^{-1} lower than the excitation bands, respectively. The vapor-phase Raman spectra show bands at 578 and 699 cm^{-1}, and these were assigned as fundamentals ν_{18} and ν_{28}, respectively.[3] The nice agreement between the Raman and SVLF spectra further confirms the assignments of the FES bands 18_0^1 and 28_0^1. The SVLF spectra with excitation of the 49_0^1 band at 326.8 cm^{-1} and of the 29_0^1 band at 329.5 cm^{-1} also nicely demonstrate the validity of our assignments. Although these two excitation bands are only 2.7 cm^{-1} from each other, there is a very obvious difference in these two SVLF spectra, as shown in Table 6, and this allows correct assignments to be made.

The eight fundamental excitation frequencies in Table 6 were compared with the corresponding frequencies from CIS/6-311++G(d,p) calculations, and were used to determine the appropriate scaling factor for the $S_1(\pi,\pi^*)$ state, as shown in Table 2. Figure 6 presents the energy level diagram for both the S_0 and $S_1(\pi,\pi^*)$ states, based on the FES and SVLF spectra.

Poential Energy Surface (PES) for the S_0 Ground State

Based upon the assignments of the low-frequency modes presented in Tables 5 and 6 and shown in Figure 6, a one-dimensional potential energy function in terms of the ring-twisting vibration was calculated. As was the case for 14BZD,[4] the barrier to inversion through the twisting mode is very high. Because the observed transitions only reach quantum states about 600 cm^{-1} above the energy minima, only the lower region of the one-dimensional PES can be determined with considerable accuracy. Hence, the estimation of the barrier by extrapolation of the potential function cannot be expected to be very accurate.

For the one-dimensional calculation the potential energy function can be described by

$$V(t) = a\tau^4 + b\tau^2 \tag{2}$$

where τ is the ring-twisting coordinate. This calculation can be done in either reduced coordinates[13] or dimensioned coordinates, and the resulting calculated transition frequencies and barriers are the same in both cases. In reduced coordinates the function that best fits the data is

$$V\,(\mathrm{cm}^{-1}) = 6.46(z^4 - 61.20z^2) \tag{3}$$

where z is the reduced coordinate. This function, which is shown in Figure 7, has a barrier to inversion of 6035 cm^{-1}, and the calculated frequencies agree well with the observed values, as shown in Table 7 and Figure 7. The coordinate z can be transformed to the dimensioned coordinate τ using[13]

$$\tau = (2\mu A)^{-(1/2)}\hbar z \tag{4}$$

where $\mu = 1/g_{44}$ is the reduced mass. The reduced mass that was calculated[13] for the simple twisting model is 32.6 au, but this large-amplitude vibration is clearly much more complicated than this model. If this reduced mass value is used, the dimensioned potential function becomes

$$V\,(\mathrm{cm}^{-1}) = (1.01 \times 10^3)\tau^4 - (4.94 \times 10^3)\tau^2 \tag{5}$$

where τ is in radians. The agreement between observed and calculated transition frequencies is again shown in Table 7. This function, however, has minima corresponding to ridiculously high twist angle values of $\pm 90°$. Part of the discrepancy apparently is related to the fact that the extrapolated barrier is 25% higher than the ab initio value of 4811 cm^{-1} and thus the minima are moved to higher τ values. The difficulty in having an accurate description of the vibrational model also contributes since a reliable reduced mass cannot readily be calculated. In addition to the twisting, the vibration no doubt also involves contributions from the out-of-plane and in-plane ring bendings as well as CH_2 motions, particularly the rocking and twisting. In order to provide some perspective on the significance of the reduced mass, a reduced mass of $\mu = 100.0$ au was arbitrarily utilized to recalculate the dimensioned potential function, and this was found to be

$$V\,(\mathrm{cm}^{-1}) = (9.48 \times 10^3)\tau^4 - (1.51 \times 10^4)\tau^2 \tag{6}$$

For this function the twisting angles are $\pm 51°$, which are much closer to the ab initio values of $\pm 31°$. However, these

TABLE 5: Frequencies (cm^{-1}) and Assignments of Single Vibronic Level Fluorescence (SVLF) Spectra of Jet-Cooled Tetralin with Excitation of the 0_0^0 band at 36 789.3 cm^{-1} [a]

this work				from ref 3		
SVLF	UV	inferred[b]	assignment	vapor IR	vapor Raman	calcd[c]
0 vs	0.0 vs		0_0^0			
−95.3 vw	−95 m		60_1^0		∼90 vw	94
−141.7 ms	−141 m		31_1^0		142 (11)	141
−256.7 vw			59_1^0		253 (1.6)	255
−283.0 m	−283 vw	283.4	31_2^0			
−306.0 w			30_1^0		298 (0.6)	301
−339.4 w			49_1^0			339
−352.1 w		352.0	$59_1^0 60_1^0$			
−397.4 vw		398.4	$31_1^0 59_1^0$			
−424.0 w, sh		425.1	31_3^0			
−428.5 m			19_1^0		427 (13)	427
−449.5 m			48_1^0		453 (2.1)	450
−480.7 vw		481.1	$31_1^0 49_1^0$			
−501.0 m			29_1^0		498 (6.2)	504
−511.6 m		513.4	59_2^0			
−524.8 vw			$58_1^0 60_1^0$			
−564.7 w, sh		566.8	31_4^0			
−569.1 m		570.2	$19_1^0 31_1^0$			
−578.0 m			18_1^0		578 (19)	581
−586.3 m			47_1^0			587
−597.0 vw		596.1	$49_1^0 59_1^0$			
−622.1 vw		622.4	$31_2^0 49_1^0$			
−641.9 w		642.7	$29_1^0 31_1^0$			
−652.5 vw		653.3	$59_2^0 31_1^0$			
−684.6 m		685.2	$19_1^0 59_1^0$			
−699.7 ms			28_1^0		699 (5.9)	703
−721.5 s		719.7	$17_1^0/18_1^0 31_1^0$		721 (83)	723
−804.0 m			46_1^0	805 w	805 (0.7)	801
−816.6 vw			27_1^0	817 w	815 (2.6)	819
−823.5 w			?			
−840.5 m		841.4	$28_1^0 31_1^0$			
−860.8 m, br		863.2/857.0	$17_1^0 31_1^0/19_2^0$			
−868.4 m			26_1^0	868 w		869
−901.1 w			56_1^0	902 w		900
−928.2 w		929.5	$19_1^0 29_1^0$			
−945.7 w		945.7	$31_1^0 46_1^0$			
−981.5 m		982.7	$28_1^0 31_2^0$			
−1005.4 m		1004.5	$17_1^0 31_2^0$			
−1035.2 s			15_1^0	1038 w	1035 (57)	1038
−1148.5 m		1150.0	$17_1^0 19_1^0$			
−1158.5 m			13_1^0		1157 (1.4)	1164
−1176.3 m		1176.9	$15_1^0 31_1^0$			
−1199.9 s			11_1^0		1199 (22)	1200

[a] Abbreviations: s, strong; m, medium; w, weak; v, very; sh, shoulder, br, broad. [b] Inferred combination frequencies are based on assignments of individual vibrations. [c] Calculated using the B3LYP/6-311++G(d,p) basis set with Gaussian 03.

calculated twisting angles have little significance since the exact description of the vibrational motion for ν_{31} is not established.

The experimental data in this case, therefore, do not do a particularly good job of determining the barrier, as they only show the barrier to be very high. The experimental results can be stated to be 6000 ± 2000 cm^{-1} for the one-dimensional model. Prediction of the twisting angle is even worse. Again only the fact that there is a large twist angle can be ascertained.

In order to account for some of the vibrational coupling involving the ring-twisting (ν_{31}) and ring-bending modes (ν_{60}), Figure 8 presents a two-dimensional graphical view, based on the ab initio calculations, of the relative energies of the twisted (T), bent (B), and planar (P) conformations. The molecule is trapped in its twisted structure, where the twisting frequency is 142 cm^{-1} and the bending frequency is 94 cm^{-1}. The molecule can undergo hindered pseudorotation and pass over a saddle point at 716 cm^{-1} corresponding to a bent configuration. This is a lower energy pathway than ascending over the planar structure at 4811 cm^{-1}.

Potential Energy Surface for the $S_1(\pi,\pi^*)$ Excited State

Similar procedures were carried out for studying the $S_1(\pi,\pi^*)$ excited state, and the data in Table 4 and Figure 6 were used. The one-dimensional potential energy function for the ring-twisting vibration in reduced coordinate is

$$V(\mathrm{cm}^{-1}) = 4.50(z^4 - 55.73z^2) \qquad (7)$$

This function has a barrier of 3487 cm^{-1} and is shown in Figure 9. This can be compared to the calculated value of 5100 cm^{-1}. However, barrier calculations for electronic excited states are

TABLE 6: Single Vibronic Level Fluorescence (SVLF) Frequencies (cm^{-1}) and Assignments from Various Fundamental Excitation Bands of Tetralin[a]

excitation assignment	0_0^0 0.0[b] vvs	31^1(B′) 94.5 vs	30^1(D′) 294.7 m	49^1 326.8 w	29^1 329.5 m	19^1 417.3 s	18^1 480.3 s	28^1 521.4 s	17^1 680.5 vs
60_1 (A)	−95 vw	−95 s							
31_1 (B)	−142 ms	−142 vs				−141 vw			−141 m
31_160_1 (A + B)		−237 w							
31_2 (2B)	−283 m	−284 m							−283 w
30_1 (D)	−306 w	−306 vw	−305 s		−305 m	−305 w			
49_1	−339 w			−339 s					
59_160_1 (A + C)	−352 w		−352 w						
31_3 (3B)	−424 w	−424 m							
19_1	−428 m				−428 m	−429 vs		−428 w	−428 w
30_131_1 (B + D)			−447 m			−447 w			
48_1	−449 m								−449 vw
31_149_1	−481 vw			−480 w					
29_1	−501 m		−501 w		−501 s	−501 w	−501 m		−501 m
59_2 (2C)	−512 w				−512 w				−512 vw
31_4 (4B)	−565 w	−565 sh							
19_131_1	−569 m	−569 w				−570 m			
18_1	−578 m	−578 w			−579 vw	−579 w	−579 s	−579 s	−578 ms
47_1	−586 m								−586 w
30_131_2 (2B + D)			−589 vw						
31_249_1	−622 vw			−621 vw					
29_131_1	−642 w				−642 vw	−643 m			
28_1	−700 ms				−701 vw	−701 m	−701 m	−701 s	
19_131_2						−712 w			
$17_1/18_131_1$	−722 s	−722 s			−721 vw		−721 m	−720 w	−721 s
28_131_1	−841 m	−841 m				−843 w			
19_2	−859 m					−858 m			
17_131_1	−862 m	−862 s							
26_1	−868 m								−864 ms
19_129_1	−928 w					−929 w			
19_159_2						−941 w			
28_131_2	−982 m	−982 w				−941 w			
$17_131_2/28_130_1$	−1005 m	−1005 w	−1007 w						−1006 m
17_130_1			−1028 m						
15_1	−1035 s	−1036 m							−1035 m
28_149_1				−1040 w					
17_149_1				−1062 m					
19_128_1						−1131 m			
17_119_1						−1152 s			
15_131_1	−1176 m	−1177							−1176 w
11_1	−1200 m	−1200							−1200 m

[a] Abbreviations: s, strong; m, medium; w, weak; v, very; sh, shoulder. [b] The excitation of 0_0^0 is at 36 789.3 cm^{-1}; the frequencies of all other excitation bands are relative to the 0_0^0.

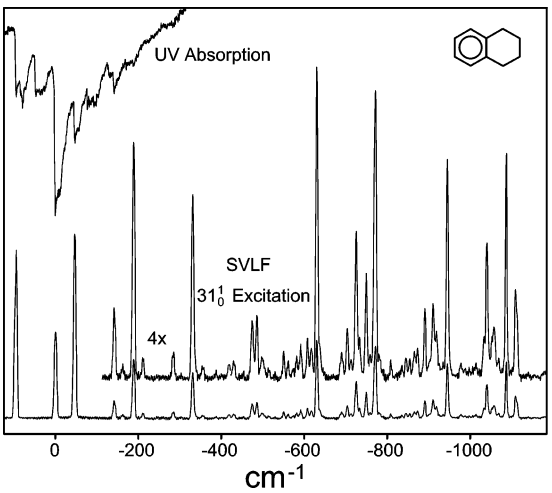

Figure 5. Single vibronic level fluorescence spectra of jet-cooled tetralin with excitation of the 31_0^1 band at 94.5 cm^{-1} above the 0_0^0 band and the ultraviolet absorption spectra at ambient temperature.

not very reliable. Table 7 also shows the agreement between observed and calculated transition frequencies.

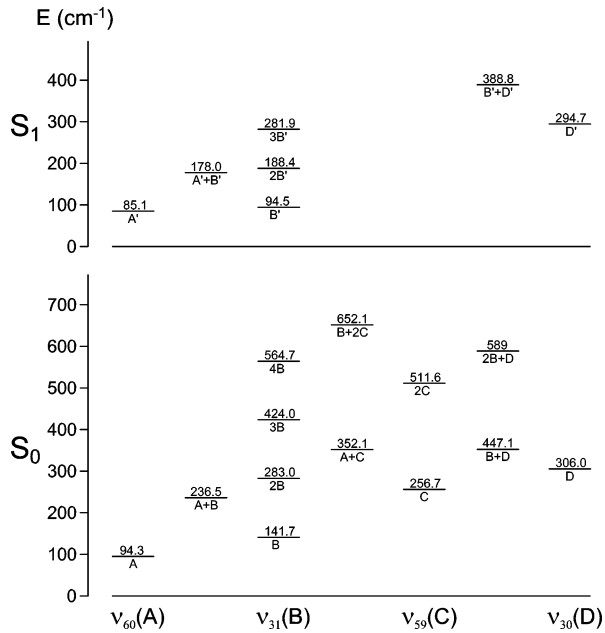

Figure 6. Energy level diagram for the low-frequency modes of tetralin in its S_0 and $S_1(\pi,\pi^*)$ states.

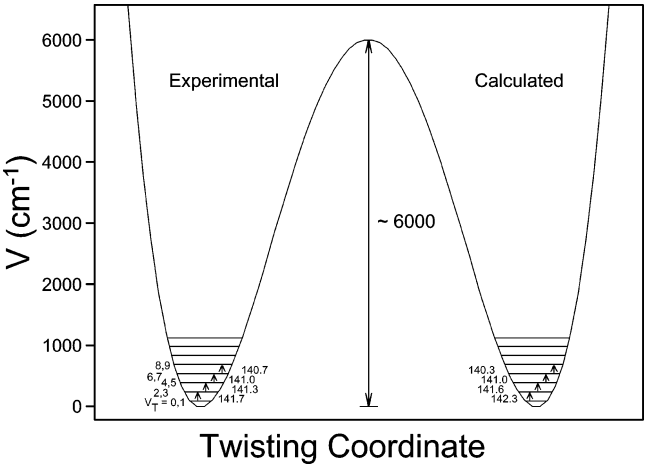

Figure 7. Experimental and calculated energy levels for the one-dimensional potential energy function of the ring-twisting vibration of tetralin in its S_0 state.

TABLE 7: Observed and Calculated Frequencies (cm^{-1}) for Twisting Transitions of Tetralin in Its S_0 Ground and $S_1(\pi,\pi^*)$ Excited States[a]

transition	obsd	calcd[b]	Δ
	S_0 ground state		
0−2	141.7 ms	142.3	0.6
2−4	141.3 m	141.6	0.3
4−6	141.0 w	141.0	0.0
6−8	140.7 w	140.3	−0.4
	S_1 excited state		
0−2	94.5 vs	94.5	0.0
2−4	93.9 m	94.0	0.1
4−6	93.5 vw	93.5	0.0

[a] Abbreviations: s, strong; m, medium; w, weak; v, very. [b] Calculated from $V = (1.01 \times 10^3)\tau^4 - (4.94 \times 10^3)\tau^2$ for S_0 state and from $V = (3.33 \times 10^2)\tau^4 - (2.16 \times 10^3)\tau^2$ for S_1 state.

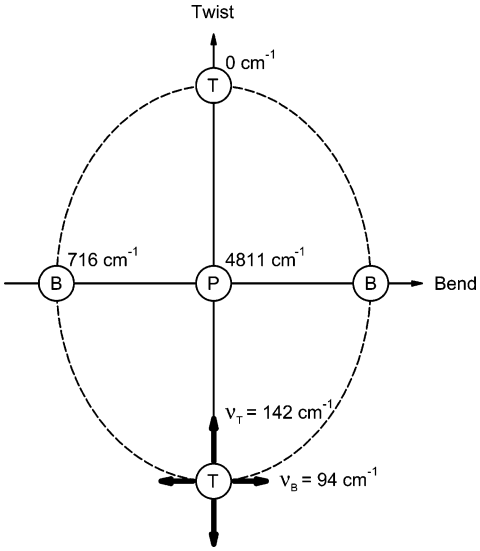

Figure 8. Representation of the two-dimensional potential energy for the ring-twisting and ring-bending vibrations of tetralin in the S_0 state. "P" = planar, "T" = twisted, and "B" = bent structure.

If the calculated reduced mass of 32.3 au is used to transfer to the dimensioned coordinate τ, the potential energy function becomes

$$V(\mathrm{cm}^{-1}) = (3.33 \times 10^2)\tau^4 - (2.16 \times 10^3)\tau^2 \qquad (8)$$

and this function has minima at ±103°, which again is ridiculously high. The arbitrary reduced mass of 100.0 au would produce twisting angles of ±58°, and the corresponding potential energy function is

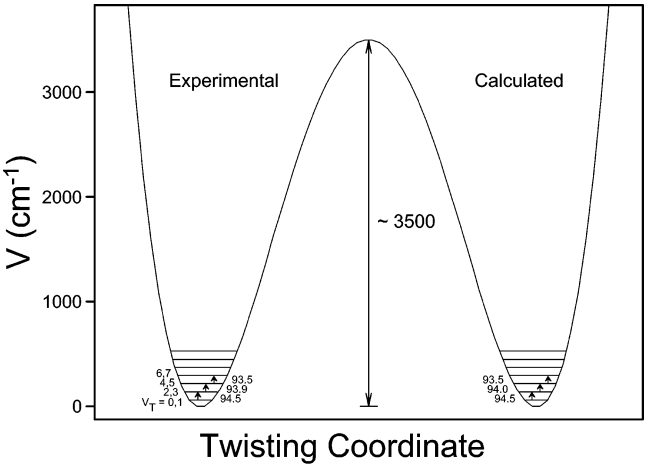

Figure 9. Experimental and calculated energy levels for the one-dimensional potential energy function of the ring-twisting vibration of tetralin in its S_1 state.

$$V(\mathrm{cm}^{-1}) = (3.20 \times 10^3)\tau^4 - (6.69 \times 10^3)\tau^2 \qquad (9)$$

An educated guess is that the S_1 excited-state barrier is about 4000 ± 2000 cm^{-1} vs 6000 ± 2000 cm^{-1} for the S_0 ground state.

Conclusions

Utilization of both spectroscopic data and computational results has allowed us to make definite assignments for many of the vibrations of tetralin in its $S_1(\pi,\pi^*)$ state as well as its ground state. For the ring-twisting vibration ν_{31}, several of the energy level spacings between quantum states have been determined but these extend to less than 1000 cm^{-1} above the ground state. Therefore, only rough estimates for the twisting barriers can be made.

Acknowledgment. The authors wish to thank the National Science Foundation (Grant CHE-0131935) and the Robert A. Welch Foundation (Grant A-0396) for financial assistance.

References and Notes

(1) Rivera-Gaines, V. E.; Leibowitz, S. J.; Laane, J. *J. Am. Chem. Soc.* **1991**, *113*, 9735.
(2) Laane, J.; Choo, J. *J. Am. Chem. Soc.* **1994**, *116*, 3889.
(3) Autrey, D.; Yang, J.; Laane, J. *J. Mol. Struct.* **2003**, *661−662*, 23.
(4) Yang, J.; Wagner, M.; Laane, J. *J. Phys. Chem. A* **2006**, *110*, 9805.
(5) Guchhait, N.; Chakraborty, T.; Majumdar, D.; Chowdhury, M. *J. Phys. Chem.* **1994**, *98*, 9227.
(6) Morris, K. Ph.D. Dissertation, Texas A&M University, 1998.
(7) Arp, Z. Ph.D. Dissertation, Texas A&M University, 2001.
(8) Arp, Z.; Meinander, N.; Choo, J.; Laane, J. *J. Chem. Phys.* **2002**, *116*, 6648.
(9) Laane, J. *J. Phys. Chem. A* **2000**, *104*, 7715.
(10) Sakurai, S.; Meinander, N.; Morris, K.; Laane, J. *J. Am. Chem. Soc.* **1999**, *121*, 5056.
(11) Frisch, M. J.; Trucks, G. W.; Schlegel, H. B.; Scuseria, G. E.; Robb, M. A.; Cheeseman, J. R.; Montgomery, J. A., Jr.; Vreven, T.; Kudin, K. N.; Burant, J. C.; Millam, J. M.; Iyengar, S. S.; Tomasi, J.; Barone, V.; Mennucci, B.; Cossi, B. M.; Scalmani, G.; Rega, N.; Petersson, G. A.; Nakatsuji, H.; Hada, M.; Ehara, M.; Toyota, K.; Fukuda, R.; Hasegawa, J.; Ishida, M.; Nakajima, T.; Honda, Y.; Kitao, O.; Nakai, H.; Klene, M.; Li, X.; Knox, J. E.; Hratchian, H. P.; Cross, J. B.; Bakken, V.; Adamo, C.; Jaramillo, J.; Gomperts, R.; Stratmann, R. E.; Yazyev, O.; Austin, A. J.; Cammi, R.; Pomelli, C.; Ochterski, J. W.; Ayala, P. Y.; Morokuma, K.; Voth, G. A.; Salvador, P.; Dannenberg, J. J.; Zakrzewski, V. G.; Dapprich, S.; Daniels, A. D.; Strain, M. C.; Farkas, O.; Malick, D. K.; Rabuck, A.

D.; Raghavachari, K.; Foresman, J. B.; Ortiz, J. V.; Cui, Q.; Baboul, A. G.; Clifford, S.; Cioslowski, J.; Stefanov, B. B.; Liu, G.; Liashenko, A.; Piskorz, P.; Komaromi, I.; Martin, R. L.; Fox, D. J.; Keith, T.; Al-Laham, M. A.; Peng, C. Y.; Nanayakkara, A.; Challacombe, M.; Gill, P. M. W.; Johnson, B.; Chen, W.; Wong, M. W.; Gonzalez, C.; Pople, J. A. *Gaussian 03*, revision C.02; Gaussian, Inc.: Wallingford, CT, 2004.

(12) Yang, J.; Laane, J. *J. Mol. Struct.* **2006**, *798*, 27.

(13) Laane, J. *Appl. Spectrosc.* **1970**, *24*, 73.